Algal Research 53 (2021) 102148

Contents lists available at ScienceDirect

Algal Research

journal homepage: www.elsevier.com/locate/algal

Effect of temperature, nitrate concentration, pH and bicarbonate addition on biomass and lipid accumulation in the sporulating green alga PW95

L. Corredor [a,b], E.P. Barnhart [c,b], A.E. Parker [b,d], R. Gerlach [b,e,f], M.W. Fields [a,b,f,*]

[a] Department of Microbiology and Immunology, Montana State University, Bozeman, MT 59717, United States
[b] Center for Biofilm Engineering, Montana State University, Bozeman, MT 59717, United States
[c] U.S. Geological Survey Wyoming-Montana Water Science Center, Helena, MT, United States
[d] Department of Mathematical Sciences, Montana State University, Bozeman, MT 59717, United States
[e] Department of Chemical and Biological Engineering, Montana State University, Bozeman, MT 59717, United States
[f] Energy Research Institute, Montana State University, Bozeman, MT 59717, United States

ARTICLE INFO

Keywords:
Microalgae
Biofuel
Lipid production
Fatty acid methyl esters (FAMEs)
Bicarbonate
Sporulating algae

ABSTRACT

The mixed effects of temperature (20 °C, 25 °C and 30 °C), nitrate concentration (0.5 mM and 2.0 mM), pH buffer, and bicarbonate addition (trigger) on biomass growth and lipid accumulation were investigated in the environmental alga PW95 during batch experiments in standardized growth medium. PW95 was isolated from coal-bed methane production water and classified as a *Chlamydomonas*-like species by morphological characterization and phylogenetic analysis (18S, ITS, *rbc*L). A factorial experimental design tested the mixed effects on PW95 before and after nitrate depletion to determine a low cost, high efficiency combination of treatments for biomass growth and lipid accumulation. Results showed buffer addition affected growth for most of the treatments and bicarbonate trigger had no statistically significant effect on growth and lipid accumulation. PW95 displayed the highest growth rate and chlorophyll content at 30 °C and 2.0 mM nitrate and there was an inverse relation between biomass accumulation and lipid accumulation at the extremes of nitrate concentration and temperature. The combination of higher temperature (30 °C) and lower nitrate level (0.5 mM) without the use of a buffer or bicarbonate addition resulted in maximal daily biomass accumulation (5.30×10^6 cells/mL), high biofuel potential before and after nitrate depletion (27% and 20%), higher biofuel productivity (16 and 15 mg/L/d, respectively), and desirable fatty acid profiles (saturated and unsaturated C16 and C18 chains). Our results indicate an important interaction between low nitrate levels, temperature, and elevated pH for trade-offs between biomass and lipid production in PW95. This work serves as a model to approach and advance the study of physiological responses of novel microalgae to diverse culture conditions that mimic environmental changes for outdoor biofuel production. The most promising conditions for growth and biofuel production were identified for PW95 and this approach can be implemented for other microalgal production systems.

1. Introduction

Green microalgae (Chlorophytes) have been the focus of major efforts towards sustainable biofuel production due to growth efficiency, ability to withstand different types of environmental stresses, and the capacity to produce value products for industrial applications [1]. Promising biofuel feedstocks have the potential to combine carbon dioxide uptake with the production of bio-oil in low quality water (e.g., coal bed methane (CBM) production water [2] or different types of wastewater [3,4]) for nutrient recycling [5]. Microalgal biofuel is derived from of triacylglycerides (TAGs) that accumulate inside the cells, which can be transesterified and converted to fatty acid methyl esters (FAMEs) [3]. FAME productivity (mg/L or mg/L/day) and profile (fatty acid (FA) chains) are used to assess a strain's potential as a biofuel producer where higher productivities in concert with lipid profiles dominated by long chain FAs (16C and 18C) are highly desirable for the biofuel industry [6].

The commercial implementation of microalgae as bio-oil/chemical feedstock, however, has been difficult to achieve. Important biological factors, such as algal strain selection, culturing strategies, the quantity and type of produced FAMEs, and the inverse relation between biomass productivity and lipid content [7] can limit production processes and

* Corresponding author at: Center for Biofilm Engineering, Montana State University, 366 Barnard Hall, Bozeman, MT 59717, United States.
E-mail address: matthew.fields@montana.edu (M.W. Fields).

https://doi.org/10.1016/j.algal.2020.102148
Received 6 December 2019; Received in revised form 21 November 2020; Accepted 22 November 2020
Available online 10 December 2020
2211-9264/© 2020 The Authors. Published by Elsevier B.V. This is an open access article under the CC BY-NC-ND license (http://creativecommons.org/licenses/by-nc-nd/4.0/).

subsequent economic viability. Frequently, green microalgal strains from culture collections such as *Chlorella* sp. [8] and *Botryococcus braunii* [9] are used to explore maximization of biodiesel potential. However, studies using native algal strains that might respond more robustly to variable growth conditions (e.g., temperature, sunlight, invasion during outdoor cultivation) are required in order to assess the viability of these biodiesel producers in different regions. The exploitation of native microalgae exposed to different physical stresses in situ that can tolerate a variety of water qualities, nutrients, and weather conditions will contribute to the advancement of microalgal biofuel systems. These environmental isolates have the potential to lower cultivation costs and increase lipid production through acclimation to local/regional fluctuating environmental conditions with low nutrient availability [1,2].

The isolation of a novel green microalga, designated strain PW95, from a CBM production wastewater pond in the Powder River Basin (northeastern Wyoming and southeastern Montana) was previously reported [2]. PW95 was shown to grow in supplemented CBM production water and to produce elevated levels of lipids for potential biofuel production but did not, however, accumulate significant levels of lipid when grown in a standardized growth medium [2]. Previous studies have demonstrated that temperature [10,11], pH buffer [12], nutrient limitation [13,14], and the addition of inorganic carbon sources such as bicarbonate [15] can have significant effects on biomass and lipid yields in different microalgae. Moreover, bicarbonate addition (i.e., trigger) has been shown to induce and/or accelerate TAG accumulation in different algae [15,16].

This study aimed to determine an optimal combination of culture conditions for low cost, sustainable biofuel production using a factorial experimental design, where growth, biofuel potential, and productivity were assessed in nitrogen replete and deplete conditions under different temperature levels (20, 25 and 30 °C), nitrate concentrations (0.5 and 2.0 mM), pH (with and without buffer) and bicarbonate addition (with and without bicarbonate trigger). The approach uses an environmental algal isolate (PW95) with a factorial experimental design that allows the evaluation of physiological responses of microalgae to diverse culture conditions (24 combinations of treatments) that mimic environmental changes for outdoor biofuel applications. Results from this study expand the knowledge of native algal isolates for use in algal biomass and lipid production systems.

2. Methods

2.1. PW95 isolation and culture maintenance

Water samples were collected from a CBM production water pond in the Powder River Basin in northeastern Wyoming (44° 52.613′N 106° 54.700′W; mean pH of 8.4 and temperature 15 °C at time of pond sampling), and plated on Bold's Basal Medium (BBM) for growth at 20 °C in a light incubator using a 14:10 h light:dark cycle (7872 lx, cool white fluorescent) and constantly shaken (125 rpm) [2]. Isolated algal colonies were transferred to liquid BBM to stimulate biomass increase. To screen for bacterial contamination, cultures were analyzed via DNA sequence analysis (SSU rRNA gene sequences). The PCR amplicons were prepared for sequencing according to the "16S Metagenomics Sequencing Library Preparation" Illumina protocol for paired-end sequencing (Illumina, San Diego, CA, USA) and sequencing was carried out using an Illumina MiSeq v3 platform. The sequence reads were processed, and bacterial operational taxonomic units identified with the MiSeq SOP pipeline of the MOTHUR software package [17]. Cultures of PW95 without bacteria were stored as stock cultures, maintained in liquid BBM at pH 8.4–8.5, and routinely checked for bacterial contamination using R2A agar plates incubated in the dark at 20 °C to check for heterotrophic growth [2].

2.2. Morphological and phylogenetic characterization of PW95

Morphological characterization of PW95 was performed using electron microscopy (EM) and epifluorescence microscopy. Sample preparation for EM was performed using centrifuged cultures (5 mL at 14,500 ×*g*), washed and resuspended in ultrapure (18.2 Ω) deionized water (dH_2O). The cell suspension (30 μL) was placed on an EM chip, and allowed to dry overnight before the chip was sputter-coated with iridium the next day. Gross morphology of PW95 was characterized using Field Emission-Scanning Electron Microscopy (Zeiss, SUPRA 55VP, Germany). Sample preparation for epifluorescence microscopy was performed by staining 1 mL of culture with 4 μL of Nile Red to observe lipid vacuoles [18] and cell mask orange for cell structure (as per manufacturer instructions; Thermo Fischer Scientific, Waltham, MA, USA). Key intracellular markers were examined using an Epifluorescence Microscope (Nikon E800 Eclipse, Model 260569, Japan) with transmitted light and fluorescence filters (B2A, TRITC, FITC). Images were captured using a digital camera (Photometrics Coolsnap, MYO, Canada).

The phylogeny of PW95 was determined by amplification, sequencing (Sanger) and comparisons of the SSU rRNA gene sequences (18S), internal transcribed sequences (ITS), and (ribulose-1,5-bisphosphate carboxylase/oxygenase (RuBisCO) large subunit (*rbc*L) sequence against the BLAST database (Basic Local Alignment Search Tool) [19]. Total genomic DNA was extracted using a Fast DNA SPIN Kit for Soil (MP Biomedicals, Irving, CA, USA). The SSU rDNA gene was amplified by PCR using the full-length primers 1-21F (5′-WACCTGGTTGTTGATCCTGCCAGT-3′) and 1741-1798R (5′-GATCCTTCYGCAGGTTCACCT-3′) and the internal primers NS3-F (5′-GCAAGTCTGGTGCCAGCAGCC-3′) and NS8-R (5′-TCCGCAGGTTCACCTACGGA-3′) [20]. Both ITS sequences were amplified as a contig with the primers ITS-1F (5′-TCCGTAGGTGAACCTGCGG-3′) and ITS-4R (5′-TCCTCCGCTTATTGATATGC-3′) [20]. The *rbc*L was amplified with the following primers: forward (5′ GATGATGARAAYATTAACTC 3′) and reverse (5′ ATTTGDCCACAGTGDATACCA 3′). PCR was performed using the following program: an initial denaturation at 94 °C for 2 min; 30 cycles at 94 °C for 30s, 57 °C for 1 min and 72 °C for 1.15 min; and a final extension at 72 °C for 7 min. The same program was used for the ITS and *rbc*L gene amplification with an increase in annealing temperature to 60 °C for the ITS and a decrease to 52 °C for *rbc*L due to the corresponding primer melting temperature (T_m). The size of each PCR amplicon was confirmed using agarose gel electrophoresis. Assembly and editing to build consensus sequences of both genes were carried out by comparing the direct and reverse chromatograms using Geneious R8 (https://www.geneious.com). The SSU rRNA gene sequence was trimmed according to sequence quality to a partial sequence (1060 bp out of 1798 bp); the ITS sequence did not require editing, and the *rbc*L sequence was trimmed for quality. Alignments for the 18S rRNA gene were conducted with the web BLASTN (Basic Local Alignment Search Tool-Nucleotide databases, https://blast.ncbi.nlm.nih.gov) and 47 DNA sequences from green algae were selected for phylogenetic analysis based on high percentages of identity (>90%) and query coverage. *Botryococcus braunii* sequences were selected as the rooted outgroup after testing tree topology and resolution with other groups of algae. The multiple sequence alignment was generated with SSU-ALIGN v0.1.1 (http://eddylab.org/software/ssu-align/) [21] based on the conserved secondary structure and sequence of the SSU rRNA and TrimAl v1.2 (http://trimal.cgenomics.org) [22] was used for automated trimming (gap threshold = 0.5). Bayesian Inference (BI) was used for phylogenetic analysis and the tree was constructed using MrBayes 3.2 (http://nbisweden.github.io/MrBayes/index.html) [23] with the following parameters: General Time Reversible (GTR) model with 8 gamma categories and 2 parallel runs, 4 chains, 2 million iterations and 0.25 burn-in fraction. iTOL v4.4.2 (Interactive Tree of Life, https://itol.embl.de) [24] was used for tree viewing, editing and annotation. To construct a BI phylogenetic tree with the ITS consensus sequence and the rbcL sequence, the same

procedure was followed as described for the 18S sequence, except the alignment was constructed with Mafft v6 [25] (BI parameters specified in Figs. S1 and S2).

2.3. Experimental design

A randomized factorial experimental design was used to determine the effect of temperature, nitrate concentration, buffer and bicarbonate addition on PW95 growth and lipid production. All experiments were performed using two independent biological replicates (repeatedly sampled every day during the duration of the growth curves) and a total of 24 treatment groups were evaluated. The experiments evaluated combinations of temperature (20, 25 and 30 °C), initial nitrate concentrations (0.5 and 2 mM), pH (with and without buffer) and bicarbonate addition (with and without bicarbonate trigger). Each treatment group has a label format consisting of all of the aforementioned factors, e.g., 20°C_0.5 Nitrate_Buffer_No Trigger, indicating the combination of temperature at 20 °C, 0.5 mM of initial nitrate, buffer and no bicarbonate addition (Fig. 1).

2.4. Experimental growth conditions

PW95 stock cultures in the exponential phase of growth, grown using identical concentrations of nitrate (0.5 or 2 mM) and environmental conditions as the experimental cultures, were used as inocula (10% of total culture volume). PW95 batch experimental cultures were grown in duplicates in conical flasks containing 200 mL of BBM with 0.5 or 2.0 mM nitrate. Nitrate concentrations were selected according to preliminary experimental trials in the laboratory. To test the effect of pH buffering, a mixture of analytical grade Trizma-Base and Trizma-HCl (Sigma-Aldrich, St Louis, MO, USA; Technical Bulletin No·106B) was added to provide a medium with an initial pH of 8.5 (identical to the pH of the unbuffered treatment). To test the effect of the bicarbonate addition, analytical grade sodium bicarbonate ($NaHCO_3$, Sigma-Aldrich,

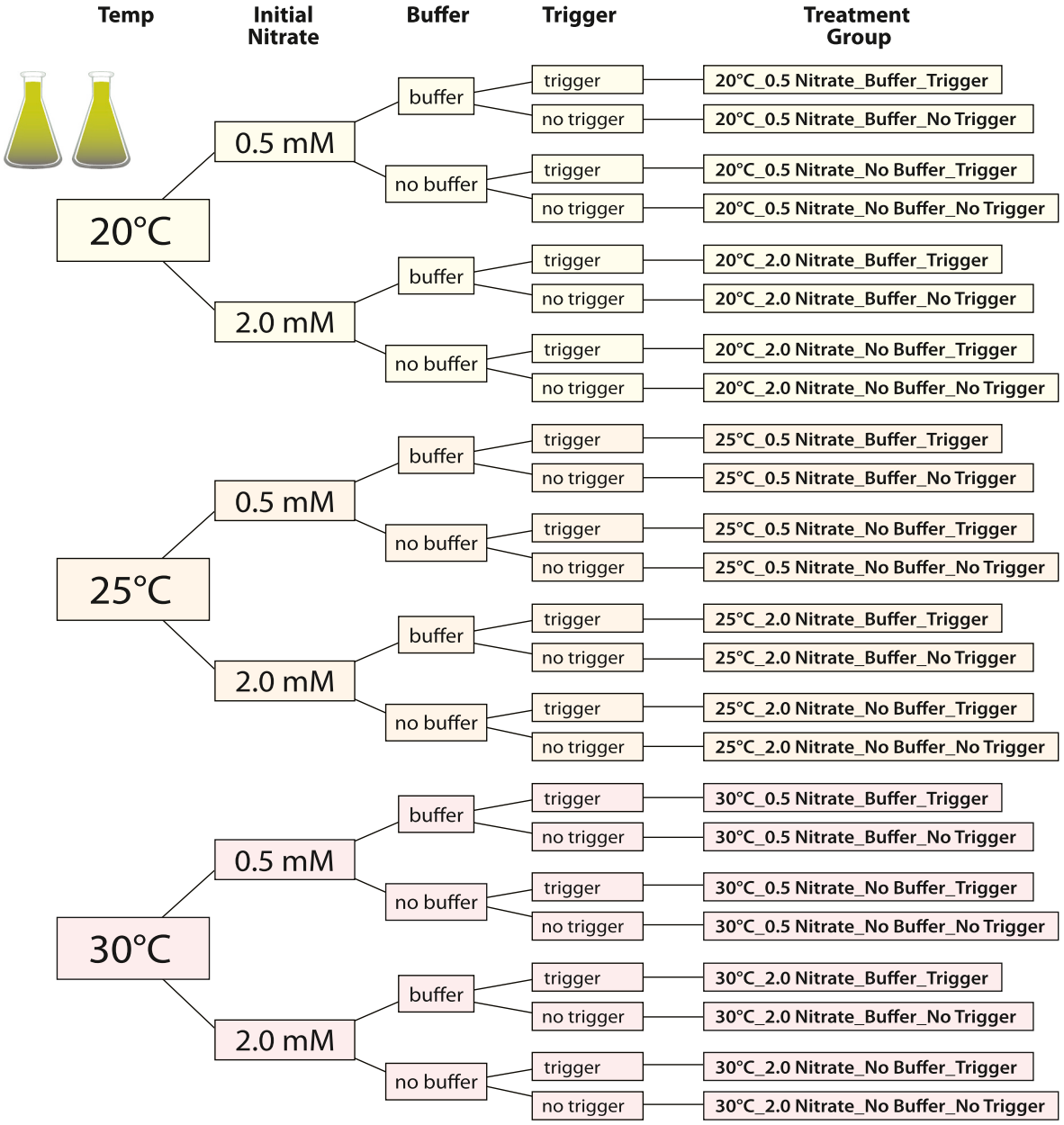

Fig. 1. Experimental design for the characterization of growth and lipid production in this study. Using a factorial design, 24 groups of treatments were evaluated and compared. All the experiments were performed using two independent biological replicates and 6 independent experiments.

St Louis, MO, USA) was added at a final concentration of 50 mM immediately before nitrate depletion as previously reported with *Chlorella vulgaris* [26]. Cultures were inoculated and grown under constant shaking (125 rpm) with gas exchange membranes as covers and a 14:10 h light/dark cycle. Light (7872 lx, cool white fluorescent) intensity was 145 μmol photons m^{-2} s^{-1}, as measured with a photosynthetically active radiation (PAR) meter (light spectra 400–700 nm, LI-COR, Lincoln, NB, USA).

2.5. Physiological response analyses

Samples were collected every 24 h immediately prior to the end of the light cycle and used for the analysis of physiological parameters. Culture pH was measured using a standard pH meter (Sension+PH1 Portable pH meter, Hach, Loveland, CO, USA). Growth performance was evaluated manually by cell counts in duplicate, using an optical hemocytometer (ThermoFisher Scientific, Waltham, MA, USA) and through chlorophyll concentration measurements. Chlorophyll was extracted using cold 100% methanol before pipetting an aliquot of the supernatant containing the extracted chlorophyll into a 96 well plate in triplicate. Chlorophyll absorbance was measured at emission wavelengths of 775 nm, 652.5 nm and 665 nm using a Synergy H1 hybrid fluorometer/spectrophotometer reader (Bio-Tek, Model H1MF, Winooski, VT, USA) [2]. Total chlorophyll concentrations (Chl-a plus Chl-b) were calculated according to Ritchie [27]. Culture (1 mL) was collected (in triplicate), centrifuged (10,625 ×*g*, 10 min, 4 °C) and the supernatant fraction was stored at −80 °C for water chemistry analysis [28]. The exogenous nitrate concentration was measured by Ion Chromatography using an AS22 Anion-Exchange Column (DIONEX ICS-1100, Dionex, Sunnyvale, CA, USA) with a 4.5 mM $NaHCO_3$/1.4 mM Na_2CO_3 buffer as eluent at a 1.2 mL flow rate with an ASRS 4 mm suppressor. A Chromeleon Chromatography Management System was used to determine the concentration of nitrate in each sample throughout the growth curve.

2.6. Lipid content analysis

Lipid content in the form of triacylglycerides (TAG) was estimated using Nile Red (NR) fluorescence as previously described [18]. Briefly, 4 μL of NR was added to 1 mL of culture and incubated for 10 min (optimal exposure time was determined using a time-course assay as reported by Chen et al. [29]). Total NR fluorescence was determined at an excitation wavelength of 530 nm and an emission wavelength of 575 nm with a Synergy H1 hybrid fluorometer/spectrophotometer reader (Bio-Tek, Model H1MF, Winooski, VT, USA) and Gen5 software.

To assess the biodiesel potential (weight of FAME/weight of biomass; w/w) of PW95, biomass samples were taken before and after nitrate depletion (Fig. S3) and before and after bicarbonate addition to examine the effect of nitrate levels and bicarbonate on PW95 lipid accumulation. Lyophilized biomass was subjected to direct in situ transesterification [30] to convert TAGs into a mixture of FAMEs or biodiesel, as follows: PW95 cultures were transferred to 50 mL sterile Falcon tubes and centrifuged (4800 ×*g* for 10 min at 4 °C). Pellets were washed twice in ultrapure deionized water (dH_2O). The supernatant was discarded, and the biomass was flash frozen at −80 °C until the samples were lyophilized. After lyophilization, biomass was weighed in glass tubes and 1 mL of toluene and 2 mL of sodium methoxide was added to the biomass. The samples were vortexed and placed in a 90 °C oven for 30 min (vortexed every 10 min). Samples were allowed to cool to room temperature and 2 mL of 14% boron trifluoride in methanol were added to each sample and vortexed. Samples were again incubated for 30 min at 90 °C and vortexed every 10 min. Samples were allowed to cool to room temperature and 0.8 mL of hexane and 0.8 mL of 15% NaCl were added to each sample. Samples were incubated for 10 min and centrifuged (2500 ×*g* for 2 min). The organic phase (top layer containing the FAMEs) was removed for quantification by Gas Chromatography–Mass Spectroscopy (GC–MS, Agilent 6890 N GC and Agilent 5973MSD, Santa Clara, CA, USA). The samples were analyzed to determine lipid concentration and composition with parameters determined by Lohman et al. [31].

2.7. Statistical analysis

Statistical analyses were performed using Minitab® Statistical Software v18 (http://www.minitab.com). To compare averages among the experimental conditions, a Linear Mixed Effects Model (LMM) [32,33] was fit to the data for each response separately (log_{10}(cells/mL), pH, chlorophyll accumulation, NR fluorescence and nitrate depletion) with: random effects for biological replicate (in a separate flask) and experiment; a covariate for time; and interactions with the fixed effects of temperature, initial nitrate, pH buffer and bicarbonate trigger. The model tested for the impact of the fixed effects after accounting for the variability among days for each biological replicate, the variability among different biological replicates, and the variability among different experiments. Tukey's follow-up tests (95% family-wise significance level) assessed all pairwise comparisons of the mean response among the treatment groups.

In cases when the linearity assumption (with respect to time) was violated, time (days) was included as a fixed effect in which case rates were not compared. Results of statistical analyses are shown as the means and standard error over multiple days of data from two independent biological replicates (i.e., flasks) and at least six independent experiments. The linearity, constant variance and normality assumptions of the LMM models employed were assessed by residual plots [33]. Assessing the constant variance assumption was crucial for our study [33]. When the data have constant variance, then the two data in each experimental group can be pooled to provide a more confident estimate of the variance and increase the power of the resulting comparisons among the means of the groups [33]. This is a common statistical approach to analyzing microbiological growth data showing high levels of variability [34].

3. Results and discussion

3.1. Morphological characterization of PW95

PW95 is a unicellular green microalga, and vegetative PW95 cells have thick cell walls, one nucleus and no flagella as observed in a variety of culture conditions (Fig. 2). NR fluorescence was used to demonstrate the accumulation of lipids (Fig. 2B), and cells showed cell-to-cell variability. PW95 is non-motile, coccoid and can be unicellular or colonial (aggregates; Fig. 2C and D). Small structures similar to cells can be observed in aggregates and based upon position and appearance, are considered to be spore-like structures or aplanospores, a form of asexual reproduction with thick cell walls and no flagella (Fig. 2E and F) [35].

3.2. Phylogenetic characterization of PW95

Algal phylogeny is complex and new isolates and sequences continue to improve the understanding of phylogenetic relatedness of eukaryotic photoautotrophs, contributing to the advancement of biofuel production systems. Bayesian phylogenetic inference using the SSU rDNA gene sequence (Fig. 3) and the ITS consensus sequence (Fig. S1), revealed that PW95 is closely related to *Chlamydomonas*-like species and members of the genera *Neospongiococcum*, *Chlamydopodium* and *Chlorococcum*, placing PW95 in the order Chlamydomonadales and grouped with non-motile coccoid green algae. Although *Chlorococcum* species show morphological similarities to PW95 vegetative cells, the SSU rRNA gene phylogenetic tree shows longer average branch lengths between *Chlorococcum* sequences and the PW95 sequence, hence a greater phylogenetic distance with *Chlorococcum* species. Further analysis using the *rbc*L fragment also indicated the closest relative to be a *Chlamydomonas* species (Fig. S2), confirming PW95 as a *Chlamydomonas*-like microalga.

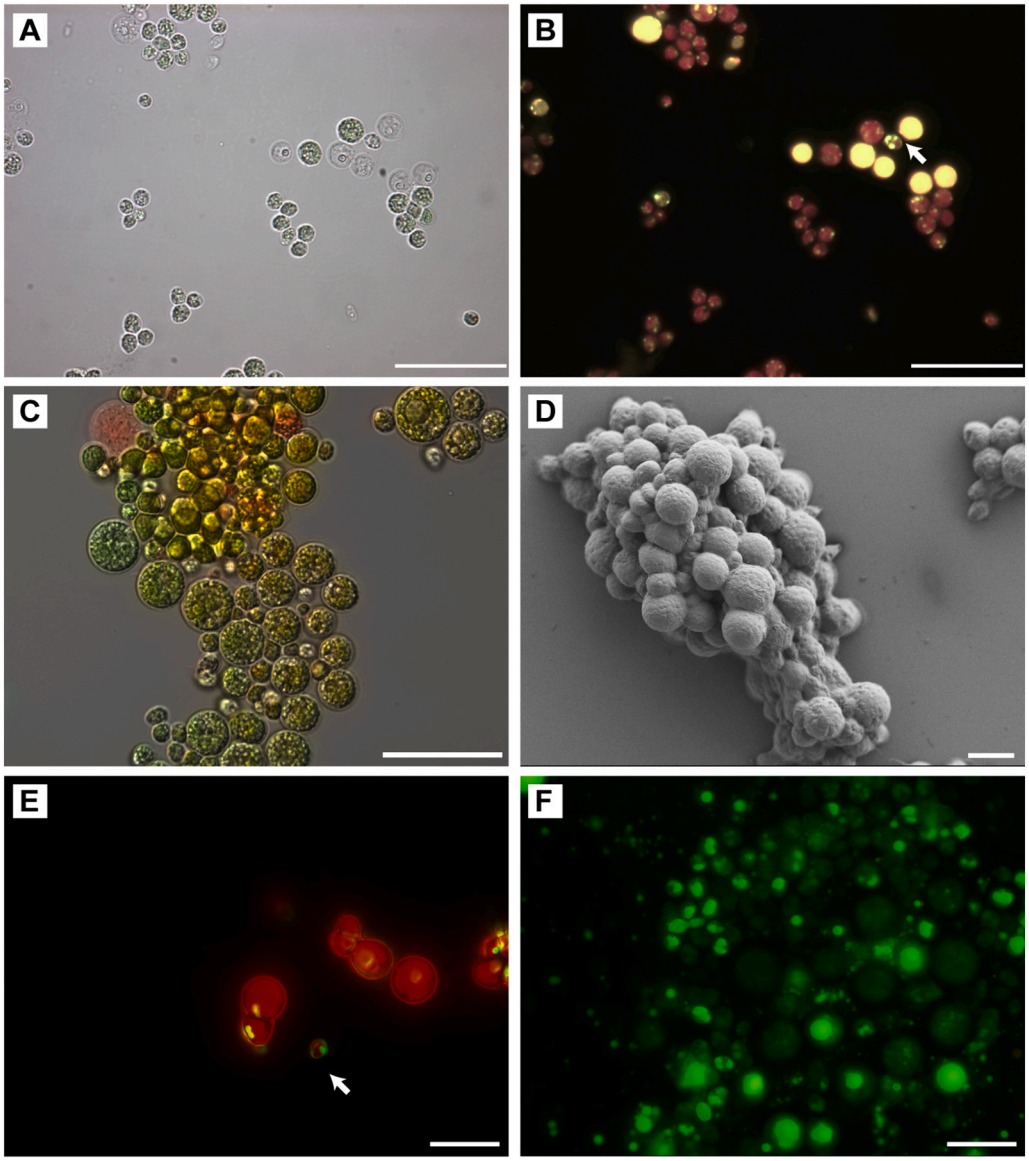

Fig. 2. Morphological characterization of PW95 native alga cultured in Bold's medium. Transmitted light microscopy (**A**) and the corresponding epifluorescence microscopy image using Nile Red stain (**B**), show different levels of lipid accumulation inside the cells (shown by yellow fluorescence, white arrow). Epifluorescence microscopy (**C**) using Cell Mask Orange (CMO), a membrane-specific dye (green), shows vegetative mature and young cells of coccoid body shape with large nuclei and thick cell walls. Images B and C also show chlorophyll auto-florescence in red. Images A, B and C at 60× show a 35 μm scale bar. FE-SEM (**D**) image at a 318× magnification with 10 μm scale bar, showing a cell aggregate of PW95 and gross cell morphology. Epifluorescence microscopy (**E**) using SYBR green, nucleic acid specific dye (green/yellow) and chlorophyll auto-florescence in red, shows vegetative mature and young cells with coccoid body accompanied by an aplanospore (white arrow), thick cell walls are observed in cells and spore at 20 μm scale. (**F**) Algal aggregate showing large vegetative cells and small aplanospores with different levels of SYBR green intensity at 10 μm scale. (For interpretation of the references to color in this figure legend, the reader is referred to the web version of this article.)

3.3. PW95 growth using different combinations of temperature, initial nitrate concentration, pH buffer addition, and bicarbonate addition

Given the novelty of the organism, we employed a factorial experimental design that allowed for a practical assessment of multiple growth and lipid production responses. We investigated each of the 24 experimental conditions with 2 independent biological replicates tested over a minimum of 4 days resulting in a minimum of 144 samples collected from a total of 48 biological replicates over 6 independent experiments (Fig. 1). Although technical replicates tend to exhibit lower variability (i.e., receive the same inoculum and are tested side-by-side on the same day), we purposely used more variable independent biological replicates over independent experiments to better reflect and account for the variability to be expected by other researchers, and predict the outcomes of future biological replicates in future experiments. The effects of temperature (20, 25 and 30 °C), initial nitrate concentration (0.5 and 2 mM), and the addition of a buffer (buffer vs. no buffer) on PW95 growth and chlorophyll production were evaluated (Figs. 4, 5 and 6). In an attempt to induce TAG accumulation, a bicarbonate 'trigger' (addition vs. no addition) was added to different experimental cultures prior to nitrate depletion and compared to the unamended cultures (Figs. 4, 5 and 6).

Temperature shifts beyond optima could have inhibitory effects on growth. Lower temperatures can decrease growth rate and higher than optimal growth temperatures have been reported to cause growth retardation and heat stress that can lead to culture collapse [36]. Previous experiments with PW95 at 15 °C and 35 °C showed poor growth and morphological evidence of stress regardless of nitrogen concentration (data not shown). These results indicated that optimal temperatures for PW95 would be above 15 °C and below 35 °C in accordance with extensive scientific literature in which the optimum temperature range for most algal species is 20–30 °C [1]. Based upon previous results [2], lipid production was higher when 0.5 mM nitrate was used for growth. Preliminary studies in the laboratory using different nitrate concentrations (3 mM (standard BBM concentration), 2 mM, 1 mM and 0.5 mM) showed that growth was similar between 3 and 2 mM nitrate under the tested conditions and that 0.5 mM performed better than 1 mM (the in situ CBM water had very low nitrate levels; data not shown). Therefore, 0.5 and 2 mM initial nitrate levels were selected as the experimental conditions.

To identify statistical differences among treatment groups, the means of log10(cell/mL) during the first 4 days of growth before the trigger were compared, as well as the means during the days after the trigger. Table 1 shows the ranking of the treatments according to this criterion,

Fig. 3. Phylogenetic relations of PW95 alga (indicated in bold) based on nuclear-encoded 18S SSU rDNA sequence comparisons. 47 sequences longer than 1000 bp were used for the analysis and the phylogenetic tree was constructed using Bayesian Inference. All Bayesian posterior probabilities are shown with colored dots on the branches. The global average standard deviation of split sequences was 0.008. *Botryococcus braunii* was chosen as outgroup (sequences shown as a collapsed clade).

and the treatments that do not share a letter are significantly different. Before the trigger, three statistically significant differences were observed: 30 °C_0.5 Nitrate_No Buffer and 30 °C_2.0 Nitrate_No Buffer had the most growth, and 25°C_2.0 Nitrate_No Buffer had a mean significantly higher than 25°C_0.5 Nitrate_Yes Buffer. After the trigger, there was only one single statistically significant difference: 30 °C_0.5 Nitrate_No Buffer had a larger mean than 25°C_2.0 Nitrate_No Buffer. Additionally, biological differences in growth were compared across treatments during the exponential growth phase based upon growth rate, doubling time and maximum daily cell density (Table 2). The top performing treatments exhibited the highest growth rates and maximum daily cell density: 30 °C_0.5 Nitrate_No Buffer_No Trigger (0.8 d^{-1}, 5.30 × 10^6 cells/mL, $p < 0.05$), 30 °C_0.5 Nitrate_No Buffer_Trigger (0.96 d^{-1}, 5.33 × 10^6 cells/mL, $p < 0.05$), 30 °C_2.0 Nitrate_No Buffer_No Trigger (1.38 d^{-1}, 6.54 × 10^6 cells/mL, $p < 0.05$; Fig. 4) and 25°C_2.0 Nitrate_No Buffer_No Trigger (1.02 d^{-1}, 1.80 × 10^6 cells/mL, $p < 0.05$). The latter, at 25 °C, stands out showing a fast growth rate (1.02 d^{-1}) but the overall performance of the culture was poor, as growth declined after day 3 (Fig. 5B). In contrast, cultures that displayed poor growth (25°C_0.5 Nitrate_Buffer_No Trigger: 0.40 d^{-1}, 6.81 × 10^5 cells/mL, $p <$ 0.05 and 25°C_2.0 Nitrate_ No Buffer_Trigger: 0.43 d^{-1}, 2.44 × 10^6 cells/mL, $p < 0.05$) appear to have high biomass production according to the maximum daily cell density (showing a sudden spike in daily growth) but the overall performance of the culture was poor with longer doubling times (17.85 h and 16.93 h, respectively; Table 2, Fig. 5A and B). The use of biological replicates across all treatments provided higher degrees of freedom that allowed the identification of statistically significant differences in means. Both the biological descriptors (Table 2) and the statistical analysis (Table 1) show that the treatments at 30 °C had the most growth and 30 °C_0.5 Nitrate_No Buffer_No Trigger was the top performing treatment in terms of growth. The other tested treatments had similar means (shared grouping, A and B) without statistically significant differences ($p > 0.05$; Table 1).

Temperature has been shown to influence algal growth, as it affects cellular metabolic rates, enzymatic activities, respiratory and photosynthetic electron transport, and other important aspects such as membrane fluidity and structure [10,37]. Overall, mesophilic temperature (30 °C) appeared to have a positive effect on PW95 growth regardless of the amount of initial nitrate ($p < 0.05$; Figs. 4A, B, 5A, B, 6A and B). At 30 °C, PW95 had a greater increase in cell numbers, a shorter lag phase (1 day) and faster growth rates in comparison with treatment groups at 20 and 25 °C (Table 2). Previous studies by Han et al. [11] observed optimum daytime temperature for *Chlorella pyrenoidosa* at 30 °C for maximum biomass and lipid production between

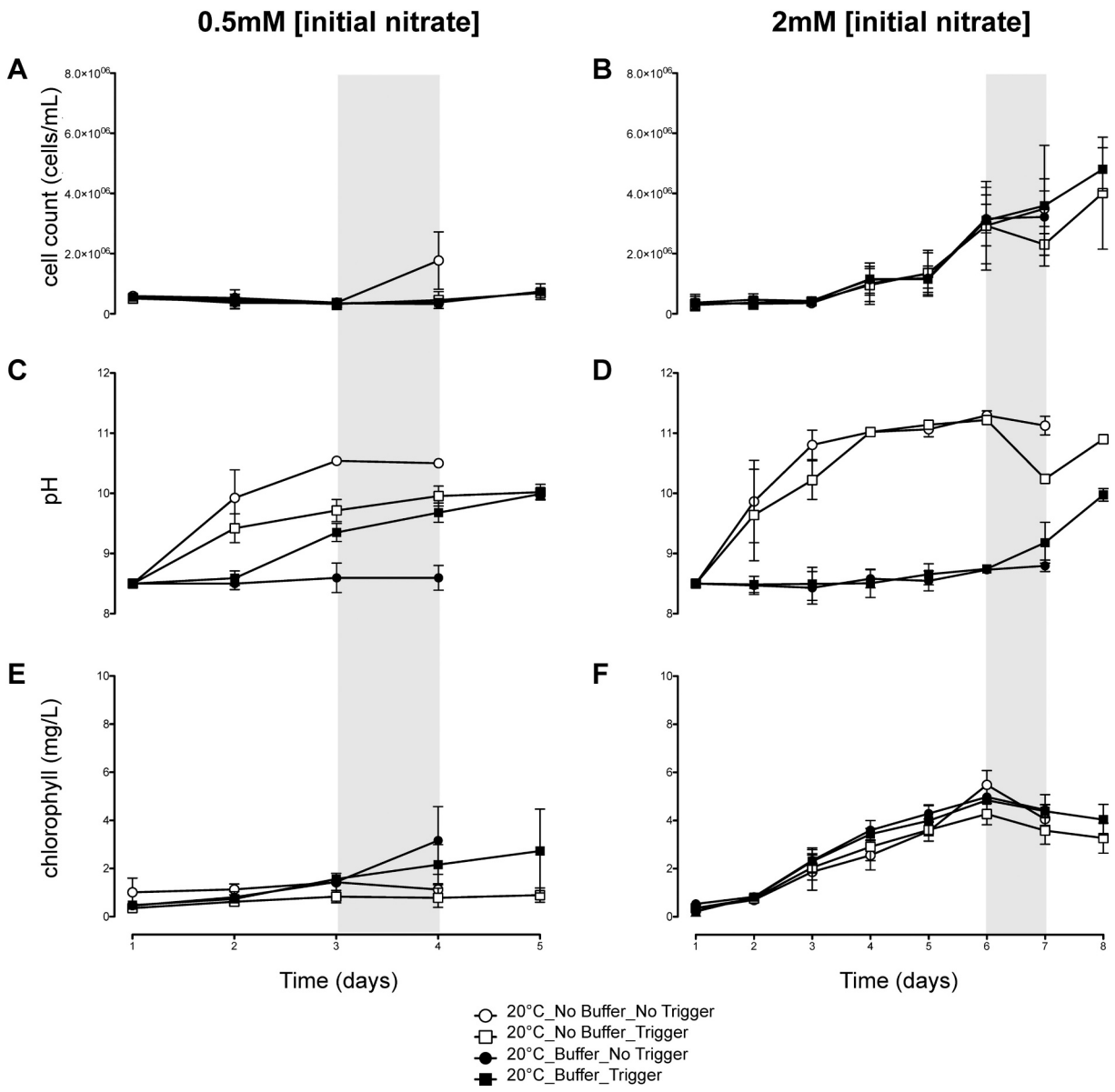

Fig. 4. Comparison between the treatment groups evaluated at 20 °C at two different concentrations of initial nitrate in terms of growth (cells/ml; A & B), media pH (C & D) and chlorophyll production (E & F). Not all the cultures arrived at nitrate depletion at the same time point, so nitrate depletion is depicted as a time frame with the shaded region in all graphs. Bicarbonate trigger, if employed, was added just prior to the onset of nitrate depletion. Filled symbols represent the combination of treatments that included the use of a buffer and the open symbols represent treatments without buffer. Treatments with trigger are represented by squares and without trigger with circles. The mean of two independent biological replicates with the standard error of the mean (error bars) is displayed in each graph.

daytime and nighttime production. Nogueira et al. [38] described higher growth rates at higher temperature when comparing growth in marine algae at 20 and 30 °C but reported no difference in overall cell density when exposed to different light intensity in combination with temperature. A similar trend was observed in *Chlorella minutissima* under minimum irradiance in which maximum growth rate increased from 0.12 d^{-1} at 10 °C to 0.66 d^{-1} at 30 °C [39]. For PW95, the interaction between higher temperature and low initial nitrate concentration was a stimulating factor for faster growth rates and maximum daily cell density (Table 2). For example, in treatments with no buffer and no trigger with 0.5 mM of initial nitrate, the growth rate increased from 0.03 d^{-1} at 20 °C to 0.8 d^{-1} at 30 °C and from a maximum daily cell density of 5.2 × 10^5 to 5.3 × 10^6 cells/mL (No Buffer_No Trigger). The lower temperatures evaluated in this investigation (20 and 25 °C) did not show significant increases in cell numbers at 0.5 mM of nitrate (Figs. 4A and 5A). At 2 mM of nitrate, an uptrend in exponential growth was observed (starting at day 5) in all the treatments at 20 °C (Fig. 4B) and these results may suggest an interdependence of nitrate utilization and temperature when nitrate and temperatures are lower. Optimum temperature for growth can be species-specific [40,41], and PW95 accumulated cells and chlorophyll the fastest at 30 °C (Fig. 6B and F). In addition, at 2 mM nitrate, a higher biomass yield (cells) was obtained at 30 °C compared to 20 °C (6.54 × 10^6 versus 3.49 × 10^6 cells/mL, respectively). Menegol et al. [14] showed a similar trend in *Heterochlorella luteoviridis* with an increase in biomass accumulation at higher temperatures (27 and 32 °C compared to 22 °C) in combination with the highest concentrations of nitrate tested by the authors.

Chlorophyll and biomass production are highly dependent on external nitrogen availability, and chlorophyll accumulation has been used previously to monitor culture health and as an alternative method for measuring biomass accumulation in different algae [42]. In addition, rapid declines in chlorophyll have been associated with nitrogen

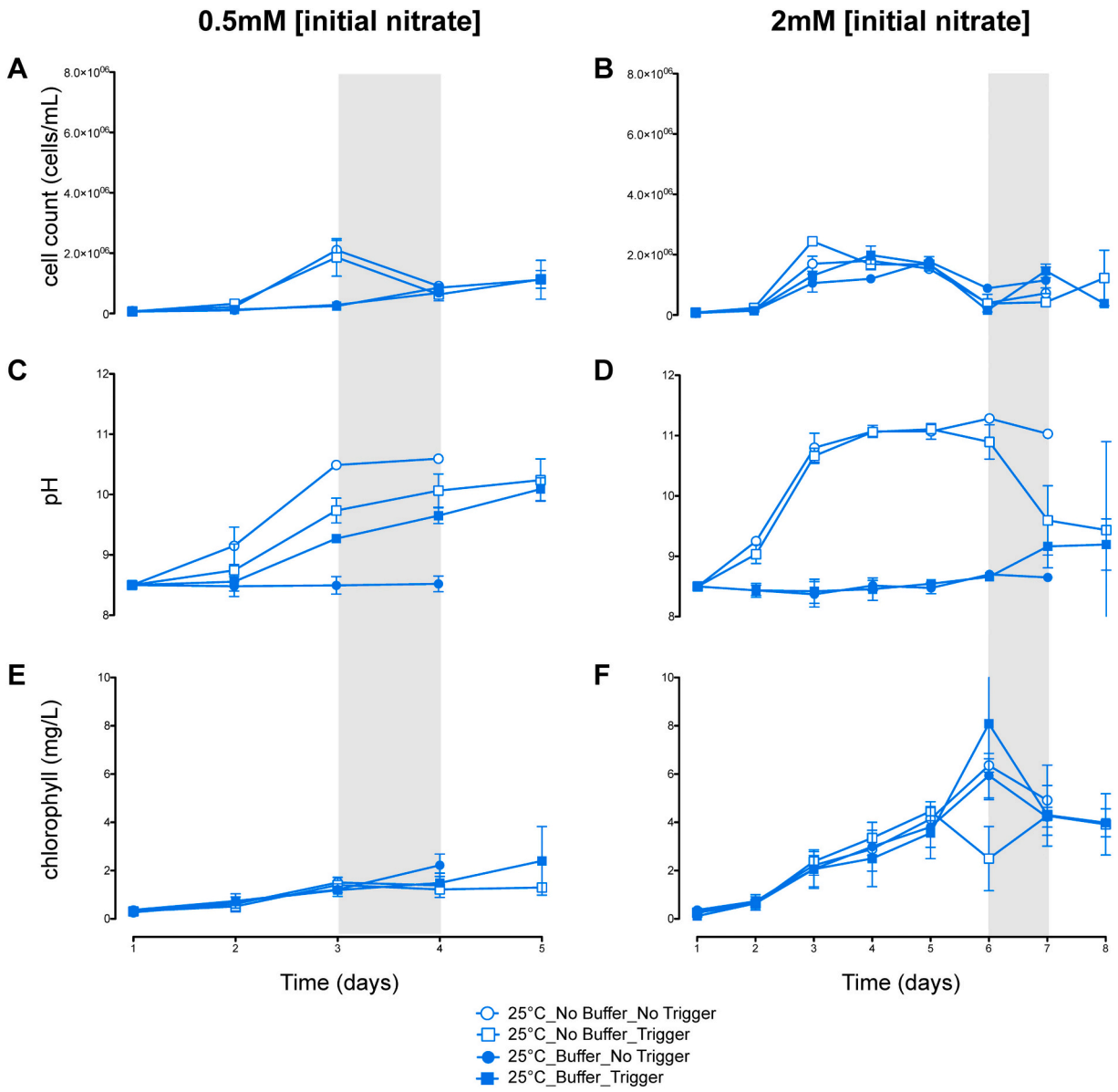

Fig. 5. Comparison between the treatment groups evaluated at 25 °C at two different concentrations of initial nitrate in terms of growth (cells/ml; A & B), media pH (C & D) and chlorophyll production (E & F). Not all the cultures arrived at nitrate depletion at the same time point, so nitrate depletion is depicted as a time frame with the shaded region in all graphs. Bicarbonate trigger, if employed, was added prior to the onset of nitrate depletion. Filled symbols represent the combination of treatments that included the use of a buffer and the open symbols represent treatments without buffer. Treatments with trigger are represented by squares and without trigger with circles. The mean of two independent biological replicates with the standard error of the mean (error bars) is displayed in each graph.

starvation [12]. As expected, PW95 had higher chlorophyll levels in cultures with 2 mM initial nitrate (2–6 mg/L chlorophyll) in comparison with the 0.5 mM cultures (1–4 mg/L chlorophyll), and similar results have been reported for PW95 in CBM production water [2] as well as for *P. cruentum* [43], *P. tricornutum* [12,44], *N. oleoabundans* [45] and other algal cultures [46]. At 0.5 mM nitrate, the 30 °C cultures had slightly higher chlorophyll levels than the cultures at 20 and 25 °C (Fig. 4E). In addition, there were not significant differences ($p > 0.05$) that could be associated with differences in growth and chlorophyll levels (Fig. 4B vs F), and these results suggested that there was no significant correlation between overall biomass and chlorophyll as has been previously reported for other alga [46]. Moreover, there was an inverse relationship between cell density and chlorophyll production, and these results indicated that chlorophyll was not a good index for growth and cell production for PW95 under the tested conditions. For example, the two treatment groups with the best growth performance at 0.5 mM nitrate (30°C_0.5 Nitrate_No Buffer_No Trigger and 30 °C_0.5 Nitrate_No Buffer_Trigger; Fig. 4A) had very low levels of chlorophyll production. In contrast, the buffered treatments showed less growth (with or without trigger) but the highest chlorophyll. The use of chlorophyll as an intracellular nitrogen pool can occur during nitrogen deprivation and has been previously reported in *N. oleoabundans* [45], *P. tricornutum* [44], and in plants where chlorophyll degradation pathways have been discovered and are considered vital for leaf senescence and fruit ripening [47]. Additionally, low chlorophyll levels can be associated with an increase in antioxidants as a possible response to reactive oxygen species (ROS) after prolonged nitrogen starvation, as reported for *Chlorella sorokiniana* [48], but the physiological responses to oxidative stress during photosynthesis in PW95 are not known. At low initial nitrate (0.5 mM), an increase in chlorophyll production started during nitrate depletion (day 3) for treatment groups with added buffer across temperatures, regardless of the presence or absence of bicarbonate

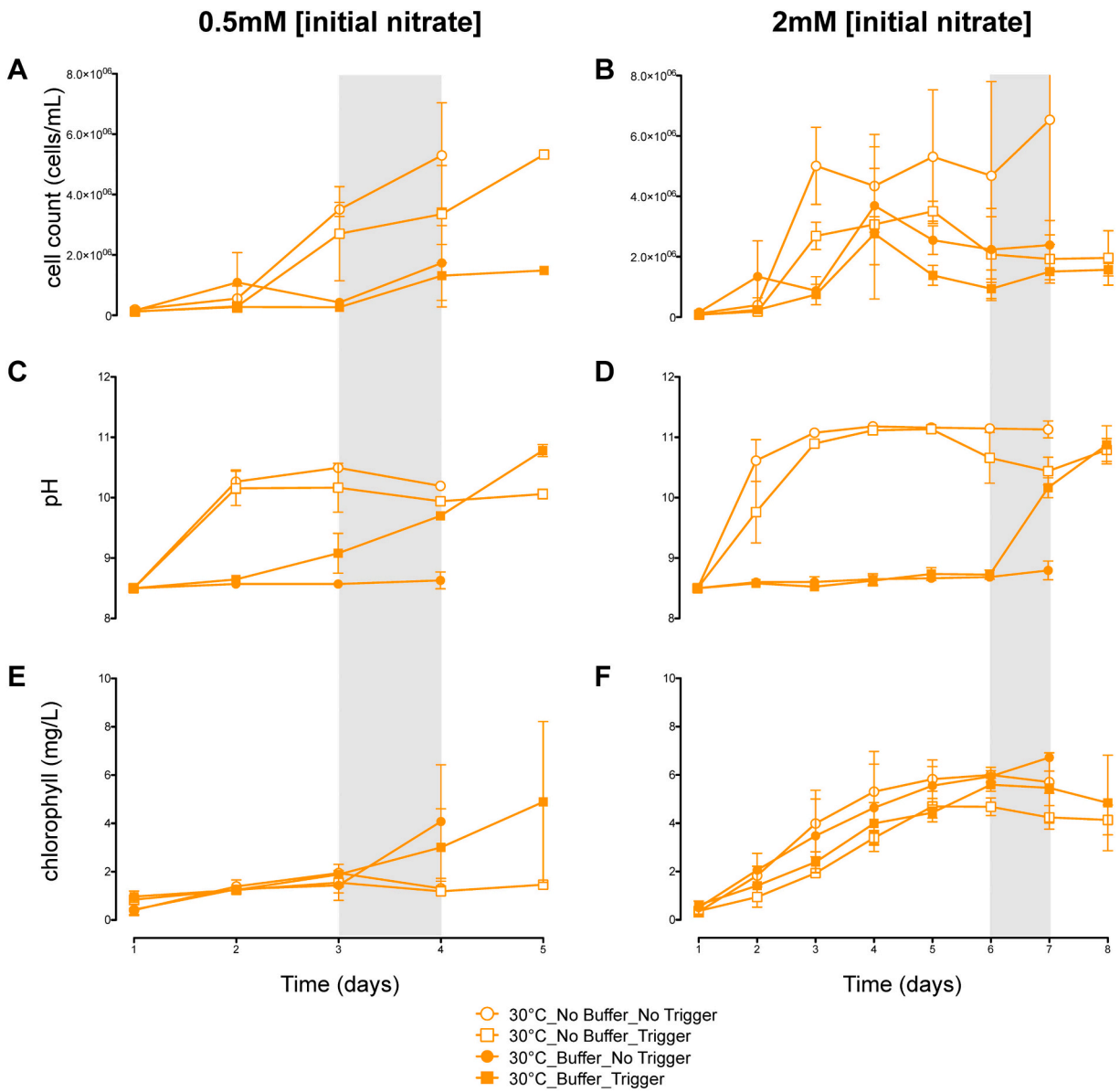

Fig. 6. Comparison between the treatment groups evaluated at 30 °C at two different concentrations of initial nitrate in terms of growth (cells/ml; A & B), media pH (C & D) and chlorophyll production (E & F). Not all the cultures arrived at nitrate depletion at the same time point, so nitrate depletion is depicted as a time frame with the shaded region in all graphs. Bicarbonate trigger, if employed, was added prior to the onset of nitrate depletion. Filled symbols represent treatments that included the use of a buffer and the open symbols represent treatments without buffer. Treatments with trigger are represented by squares and without trigger with circles. The mean of two independent biological replicates with the standard error of the mean (error bars) is displayed in each graph.

(Figs. 4, 5 and 6). Although this change was not statistically significant ($p > 0.05$), it can be argued that resources were being allocated as a reserve for a potential 'persistent state' in response to the nitrogen (N) depletion. Green algae, such as *Chlamydomonas* and *Volvox*, produce morphologically distinct spores for this purpose [49]. PW95 is an environmental isolate that could possibly have a sporulating resting stage triggered by specific environmental conditions, such as pH level and nutrient starvation. Further work is needed to better understand the role of spores in the life cycle of PW95 and how different sporulating green alga overall respond and survive nutrient deprivation in terms of biomass accumulation.

Previous studies have shown that bicarbonate supplementation in combination with nitrogen starvation at lower temperatures (20–25 °C) can enhance cell division, increase biomass and desired biochemical composition in marine algae [12] and chlorophytes such as *Scenedesmus* sp. [50] and *Chlamydomonas reinhardtii* [15]. However, bicarbonate did not significantly affect PW95 growth and biomass accumulation under the tested conditions. Treatments at 2 mM nitrate and 25 °C with and without buffer exhibited higher cell counts (Fig. 5B), but the comparison with no bicarbonate counterparts revealed no significant difference ($p > 0.05$; Table 2). The presence of bicarbonate after nitrate depletion did not appear to have a positive effect on growth and biomass accumulation, and further work is needed to investigate inorganic carbon utilization in PW95 and elucidate the potential activation of carbon (C) concentrating mechanisms when bicarbonate is present in the medium.

The pH was monitored daily to assess changes due to carbon fixation [51] and the effect of pH control with buffer addition on growth and lipid accumulation. As expected, culture pH increased for cultures with significant activity most likely due to nitrate and CO_2 utilization during photosynthesis. At each tested temperature, pH increased to between 9 and 10 during initial growth for both nitrate levels (0.5 and 2 mM) and approached approximately 10.5 as nitrate was depleted for the 0.5 mM

Table 1
Ranking of experimental conditions by the mean $\log_{10}$(cell/mL). Before the bicarbonate addition, the mean $\log_{10}$(cell/mL) was calculated during the first 4 days of growth; after the bicarbonate addition, mean $\log_{10}$(cell/mL) was calculated to day 8. SEM indicates standard error of the mean. Statistically significantly ($p < 0.05$) different treatments do not share a letter.

Bicarbonate trigger	Temperature (celsius)	Initial nitrate (mM)	pH buffer	N	Mean	SEM	Grouping
Before[a]	**30**	**0.5**	**No**	**13**	**5.90**	**0.14**	**A**
	30	**2**	**No**	**16**	**5.78**	**0.11**	**A**
	20	0.5	No	12	5.75	0.10	A,B
	30	2	Yes	16	5.64	0.11	A,B
	20	2	Yes	16	5.63	0.10	A,B
	25	**2**	**No**	**16**	**5.61**	**0.06**	**A**
	20	0.5	Yes	12	5.60	0.06	A,B
	20	2	No	16	5.57	0.07	A,B
	25	0.5	No	12	5.56	0.09	A,B
	30	0.5	Yes	13	5.54	0.15	A,B
	25	2	Yes	16	5.49	0.06	A,B
	25	**0.5**	**Yes**	**12**	**5.24**	**0.05**	**B**
After	25	2	Yes	4	7.01	0.07	A,B
	30	**0.5**	**No**	**5**	**6.90**	**0.12**	**A**
	20	2	Yes	6	6.40	0.11	A,B
	30	0.5	Yes	5	6.37	0.23	A,B
	20	2	No	6	6.33	0.18	A,B
	25	0.5	Yes	6	6.22	0.12	A,B
	30	2	No	6	6.14	0.27	A,B
	30	2	Yes	4	6.14	0.05	A,B
	20	0.5	No	6	5.92	0.17	A,B
	20	0.5	Yes	6	5.89	0.07	A,B
	25	0.5	No	6	5.86	0.14	A,B
	25	**2**	**No**	**6**	**5.43**	**0.18**	**B**

[a] Up to 4 days before the trigger.

Table 2
Comparison of growth characteristics among all treatment groups. Values are reported as the mean of two independent biological replicates with standard errors for the growth rate and mean cell number.

Temp (celsius)	Initial nitrate (mM)	pH buffer	Bicarb trigger	Growth rate (day^{-1})	Doubling time (hours)	Max daily cell number (cells/ml)	
20	0.5	No	No	0.03 ± 0.02	(n/a)	5.19E+05	±8.8E+02
			Yes	0.09 ± 0.03	(n/a)	1.66E+05	±8.3E+04
		Yes	No	-0.10 ± 0.06	(n/a)	5.51E+05	±3.4E+04
			Yes	0.07 ± 0.02	(n/a)	7.40E+05	±1.8E+05
	2	No	No	0.45 ± 0.16	16.08	3.49E+06	±6.7E+05
			Yes	0.37 ± 0.13	19.59	4.01E+06	±1.3E+06
		Yes	No	0.41 ± 0.15	17.44	3.22E+06	±9.0E+05
			Yes	0.43 ± 0.15	16.72	4.80E+06	±5.1E+05
25	0.5	No	No	0.71 ± 0.51	10.11	2.10E+06	±8.0E+05
			Yes	0.76 ± 0.27	9.51	1.86E+06	±4.4E+05
		Yes	No	0.40 ± 0.29	17.85	6.81E+05	±9.3E+04
			Yes	0.27 ± 0.10	26.45	1.12E+06	±4.6E+05
	2	No	No	1.02 ± 0.36	7.10	1.80E+06	±8.0E+04
			Yes	0.43 ± 0.30	16.93	2.44E+06	±5.3E+03
		Yes	No	0.37 ± 0.39	19.54	1.78E+06	±5.3E+04
			Yes	0.68 ± 0.48	10.64	1.87E+06	±2.1E+05
30	0.5	No	No	0.80 ± 0.28	9.04	5.30E+06	±1.2E+06
			Yes	0.96 ± 0.34	7.53	5.33E+06	±3.5E+00
		Yes	No	0.83 ± 0.29	8.70	1.74E+06	±8.8E+05
			Yes	0.34 ± 0.12	21.50	1.31E+06	±7.3E+05
	2	No	No	1.38 ± 0.49	5.23	6.54E+06	±2.9E+06
			Yes	0.76 ± 0.54	9.53	3.51E+06	±2.3E+05
		Yes	No	0.92 ± 0.32	7.88	3.69E+06	±1.4E+06
			Yes	0.57 ± 0.20	12.74	2.76E+06	±1.5E+06

(n/a) stands for not applicable when the growth was not exponential, or the growth rate had a negative value.

nitrate treatments (Figs. 4C and D). The change in pH at 0.5 mM nitrate is similar to previous results when PW95 was grown in CBM water amended with macro- and micronutrients [2]. The 2 mM nitrate treatments were at pH 11 as nitrate was depleted (Fig. 4D), and the groups of treatments without bicarbonate trigger were significantly different ($p < 0.05$) from the triggered treatments. These results demonstrate a buffering effect of bicarbonate in PW95 cultures, as it has been used previously for pH control in algal cultures [51]. The addition of bicarbonate took place pre-nitrate depletion (shaded area in Figs. 4, 5 and 6), and statistically significant differences ($p < 0.05$) were observed among treatment groups with bicarbonate trigger. In addition, the cultures showed a pH decline for unbuffered conditions and a pH increase for the buffered conditions (Figs. 4D, 5D and 6D). The presence of bicarbonate after nitrate depletion had an effect on pH levels but not growth in PW95 cultures. Previous results reported pH control as an effective strategy for maintaining optimal growth of algal biomass during nitrogen replete conditions [51,52] but PW95 exhibited a different response. As a general trend, pH control using buffer (Trizma) addition to the medium had an

inhibitory effect on PW95 growth for most of the tested treatment combinations, and these results corresponded to a similar response reported by Mus et al. [12] when *Phaeodactylum tricornutum* cultures were buffered with TRIS at pH 8.5 and 9.0.

The effect of bicarbonate addition during nitrogen depletion on buffered cultures has been previously described in *Nannochloropsis gaditana* [15] and showed lower cell density at nitrate depletion with additional supplementation of bicarbonate, as was the case for PW95 at 30 °C regardless of initial nitrate concentration. In comparison at 20 °C, overall cell density was low with or without the use of buffer. The presented results suggest that buffer conditions could temper any possible benefit of bicarbonate addition. However, the response might be genus-, species- and even strain-dependent and further work is needed to better characterize the mechanisms by which dissolved inorganic carbon species (e.g., bicarbonate) are assimilated in PW95 and other photoautotrophs under different conditions.

3.4. Lipid analysis and effect of bicarbonate trigger on PW95 lipid production

Lipid analysis was performed by monitoring TAG accumulation using NR fluorescence (Fig. 7) and direct transesterification of TAGs into FAMEs (Fig. 8) to account for biofuel potential and to determine biofuel productivity. An increased production of lipids has been reported under nitrogen limitation, different temperatures, drastic fluctuations in pH and different combinations of these conditions [13,40]. The start of significant TAG accumulation has been frequently correlated with the onset of nitrate depletion in green algae [53,54], diatoms [44] and PW95 microalga in amended low quality water [2]. At 0.5 mM nitrate, an increase in NR fluorescence was observed at the onset of nitrate depletion and on the last day (maximum increase in fluorescence) of culturing for the following treatment groups: 30 °C_0.5 Nitrate_No Buffer_No Trigger (800 rfu), 30 °C_0.5 Nitrate_No Buffer_Trigger (1500 rfu) and 20°C_0.5 Nitrate_No Buffer_ Trigger (1000 rfu; Fig. 7A). At 30 °C, both treatment groups showed similar but not significant increases ($p > 0.05$). In contrast, the 20 °C treatment (triggered with bicarbonate) was statistically significant ($p < 0.05$; Fig. 7A). At 2 mM nitrate, increases in NR fluorescence were also observed for all treatments at 20 °C and the no buffer treatments at 30 °C. The treatment group 30 °C_2.0 Nitrate_No Buffer_No Trigger had an increase in NR fluorescence during nitrate replete conditions (days 3–6) instead of nitrate depletion but was not statistically significant ($p > 0.05$). Treatments at 25 °C also showed slight increases in NR fluorescence during nitrate replete conditions (Fig. 7B). Even though nitrogen limitation is one of the most studied strategies to increase lipid accumulation [55], we also investigated lipid accumulation before nitrate depletion (N-sufficient). Microalgae species could potentially change carbon storage patterns in favor of neutral lipids (mainly TAGs) under N-sufficient conditions in concert with optimal temperatures and pH levels. This would enable biomass collection both at N-deplete and N-replete conditions, increasing the lipid yield of the algal production system.

Previous studies have shown that the addition of different concentrations of bicarbonate in combination with nitrate depletion causes species-specific differences in lipid accumulation in *Chlamydomonas reinhardtii* [56], marine species and diatoms [42,52]. This was not the case for PW95, where the expected statistically significant increase in TAG accumulation (NR fluorescence) and FAMEs with a high concentration bicarbonate addition (50 mM) was not observed. When paired with pH control strategies, the addition of bicarbonate, such as the one used in this study, improved lipid content in *N. gaditana* [15] but this was not the case for PW95. At 0.5 mM initial nitrate, the addition of buffer had no effect on TAG accumulation and bicarbonate addition appeared to only slightly increase TAG accumulation at 20 and 30 °C by the end of the growth curve. Treatment groups with 2 mM initial nitrate at 20 °C and 30 °C did show increases in TAG accumulation during the last 2 days of culturing for the conditions that had both buffer and bicarbonate but statistical significance ($p > 0.05$) was not observed for either case (Fig. 7).

Direct in situ transesterification was used to determine the fatty acid content of the biomass and estimate the biodiesel potential without prior lipid extraction [6]. The total FAME levels before and after nitrate depletion and bicarbonate trigger were determined for the different treatments. In *C. vulgaris* [26] and other microalgae [57,58] total FAMEs can range between 10 and 60%. For PW95, a comparison of total FAMEs

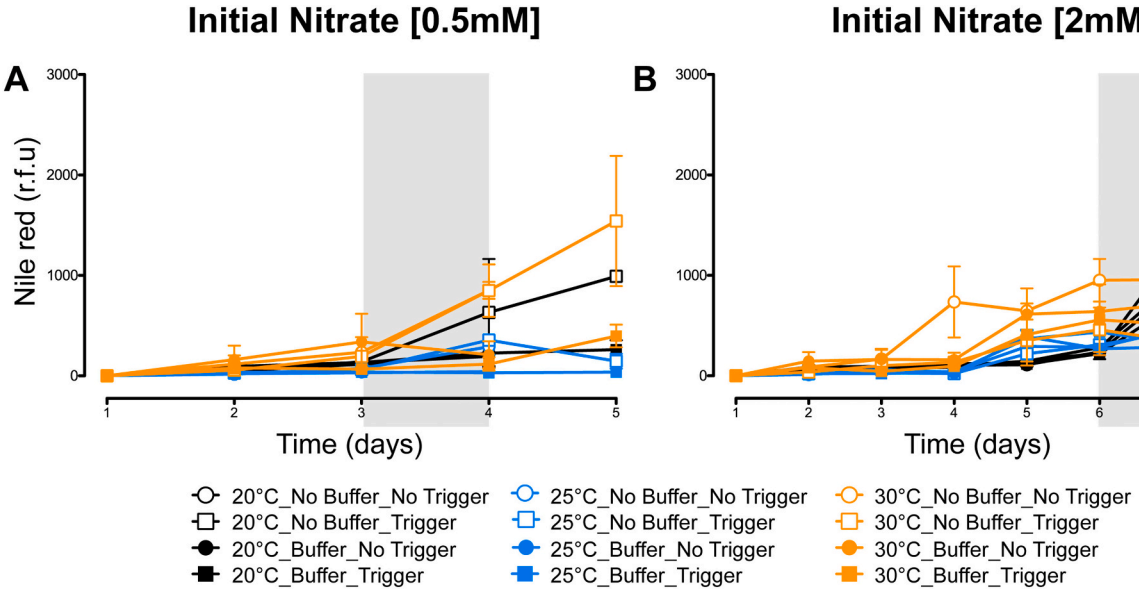

Fig. 7. Daily lipid accumulation estimated by NR fluorescence during growth of all the treatment groups evaluated in this study at 0.5 mM (A) or 2 mM (B) initial nitrate concentration. Temperatures are differentiated by color: 20 °C (**black**), 25 °C (**blue**) and 30 °C (**orange**). Not all the cultures arrived at nitrate depletion at the same time point, so nitrate depletion is depicted as a time frame with the shaded region in all graphs. Filled symbols represent the treatments that included the use of a buffer and the open symbols represent treatments without buffer. Treatments with trigger are represented by squares and without trigger with circles. The mean of two independent biological replicates with the standard error of the mean (error bars) is displayed in each graph. (For interpretation of the references to color in this figure legend, the reader is referred to the web version of this article.)

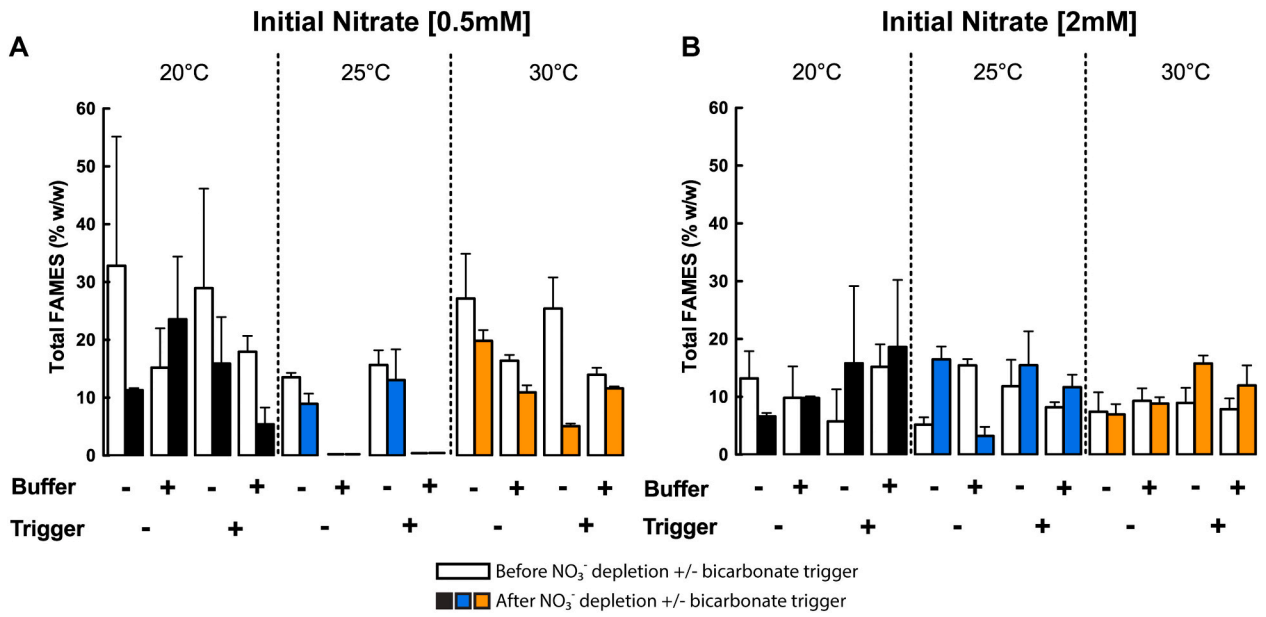

Fig. 8. Percentage of total FAMEs before and after nitrate depletion and bicarbonate trigger. The concentration of nitrate in the samples was measured daily to predict the time of nitrate depletion for biomass collection and subsequent transesterification. For treatments with bicarbonate trigger, addition of bicarbonate took place prior to the onset of nitrate depletion and biomass for transesterification was collected before and after the bicarbonate addition. The means of two independent biological replicates with the standard error of the mean (error bars) are displayed in each graph.

across treatments showed that the highest total FAME production (~30%) was observed at 0.5 mM nitrate and 20 °C without buffer or trigger and the lowest total FAME levels were observed for treatments at 25 °C (Fig. 8). When nitrate was increased (2 mM), none of the tested conditions had total FAMEs above 20% (Fig. 8b). Moreover, when total FAME levels were compared to the rate of cell or chlorophyll accumulation, chlorophyll accumulation rate was a better predictor of overall FAME production under unbuffered conditions ($R = 0.82$). These results suggest an important interaction between low nitrate levels, temperature, and elevated pH for trade-offs between biomass and lipid production in PW95. Moreover, chlorophyll accumulation may be an indicator of resource allocation during C:N imbalance (i.e., nitrogen (N) storage into chlorophyll as a prerequisite to lipid accumulation during surplus carbon (C) and/or sufficient chlorophyll to deal with prolonged light stress during N starvation).

Among the treatment groups with the highest FAME levels (20–30%; 20°C_0.5 Nitrate_No Buffer_No trigger, 20°C_0.5 Nitrate_No Buffer_Trigger, 30 °C_0.5 Nitrate_No Buffer_No trigger and 30 °C_0.5 Nitrate_No Buffer_Trigger), the general trend showed that the percentage of FAMEs was always higher before nitrate depletion. These results indicated that in treatments with a bicarbonate trigger, the percentage of FAMEs is lower after nitrate depletion/bicarbonate trigger. The bicarbonate trigger had little effect on lipid accumulation in PW95 and did not result in statistically significant differences ($p > 0.05$) in any of the treatment groups in terms of FAME levels. These results may suggest that different concentrations of bicarbonate should be examined to better understand how bicarbonate is assimilated in PW95 and if there is a specific concentration and/or type of dissolved inorganic carbon species for improved biomass and lipid accumulation in PW95.

Biofuel productivity (mg/L/day) was compared between temperatures that showed treatments with higher biofuel potential (20 and 30 °C) and the results show differences in productivity between bicarbonate trigger cultures versus the non- triggered counterparts with and without buffer (Table 3). The 20°C_2.0 Nitrate_No Buffer_Trigger, 20°C_2.0 Nitrate_Buffer_Trigger, 30 °C_2.0 Nitrate_No Buffer_Trigger and 30 °C_2.0 Nitrate_Buffer_Trigger samples showed that the bicarbonate treatments (with and without buffer) increased biofuel productivity after nitrate depletion and bicarbonate addition for both levels of initial nitrate. A potential interaction between nitrate limitation and bicarbonate addition may exist for the increase in lipid productivity but the differences before and after the bicarbonate addition were not statistically significant ($p > 0.05$). Further work is needed to determine the optimal concentration of bicarbonate trigger to stimulate lipid accumulation in nitrate deplete conditions without compromising biomass production in PW95.

Among all tested conditions, the highest biofuel productivity was observed in the 30 °C_0.5 Nitrate_No Buffer_No trigger treatment before (16.4 mg/L/day) and after (15.1 mg/L/day) nitrate depletion, with the

Table 3
Biofuel productivity comparison between treatments at 20 °C and 30 °C. Average biofuel productivity is calculated under replete conditions (prior to nitrate depletion) and deplete conditions (post nitrate depletion) and bicarbonate trigger taking into account the number of culturing days up to biomass sampling.

Temperature (C)	Initial nitrate (mM)	pH buffer	Bicarb trigger	Average biofuel productivity[a] (mg/L/day)	
				Replete	Deplete
20	0.5	No	No	14.4	4.8
			Yes	12.3	12.5
		Yes	No	7.1	14.1
			Yes	7.6	4.0
	2	No	No	7.4	2.5
			Yes	2.8	14.5
		Yes	No	5.9	7.4
			Yes	8.2	15.2
30	0.5	No	No	16.4	15.1
			Yes	9.3	5.2
		Yes	No	13.2	8.6
			Yes	5.2	12.7
	2	No	No	4.9	5.5
			Yes	5.2	15.9
		Yes	No	5.6	6.3
			Yes	5.1	15.0

[a] The biofuel productivity was using the equation for biodiesel content [12] divided by the number of culturing days up to the day of biomass collection.

Table 4
Comparison between the best performing treatments in terms of lipid accumulation at 20 °C and 30 °C. Total biofuel potential and productivity are calculated under replete and deplete nitrate conditions and bicarbonate trigger. Total biofuel potential is expressed in percentage of FAMEs.

Temp (celsius)	Initial nitrate (mM)	pH buffer	Bicarb trigger	Max daily cell number (cells/mL)	Growth rate (day^{-1})	Biofuel potential (%)		Biofuel Productivity[a] (mg/L)		Biofuel Productivity[b] (mg/L/d)	
						Replete	Deplete	Replete	Deplete	Replete	Deplete
20	0.5	No	No	5.19E+05	0.03	33	11	43	19	14	5
			Yes	1.66E+05	0.09	29	16	25	56	12	13
30	0.5	No	No	5.30E+06	0.80	27	20	41	60	16	15
			Yes	5.33E+06	0.96	25	5	23	23	9	5

[a] The biofuel productivity as concentration was calculated using equation for biodiesel content [12].
[b] Biofuel productivity as a function of time was calculated using the number of culturing days up to the day of biomass collection.

added value of producing high cell numbers at a fast growth rate, high biofuel productivity, as well as one of the highest biofuel potentials (both before and after nitrate depletion; Table 4). Although, there were other treatments with just as high biofuel potential at 20 °C, the productivities were lower in comparison with 30 °C_0.5 Nitrate_No Buffer_No trigger and there was a strong correlation between high biofuel potential and very low biomass productivity at 20 °C and 0.5 mM initial nitrate. Cell density for the treatment groups 20°C_0.5 Nitrate_No Buffer_No trigger and 20°C_0.5 Nitrate_No Buffer_Trigger was low (Fig. 4A and Table 4) but showed the highest percentage of total FAMEs, 33% and 29%, respectively (Fig. 8A and Table 4). This inverse relation between biomass and lipid accumulation has been frequently reported in the literature [7], and these results suggest that biomass accumulation was inhibited for the production of energy storage molecules. In contrast, at 30 °C and 0.5 mM nitrate, PW95 showed the highest cell density during growth (Figs. 4, 5 and 6 and Table 4) in concert with high lipid production. The percentage of total FAMEs for 30 °C_0.5 Nitrate_No Buffer_No trigger was 27% (Fig. 8A and Table 4), indicating a positive interaction between a low concentration of initial nitrate and higher temperature. Table 4 shows a summarized comparison of the aforementioned treatments and 30 °C_0.5 Nitrate_No Buffer_No trigger was the best performing treatment under the tested conditions, producing high levels of biomass and lipids in a short period of time.

Lastly, when PW95 lipid profiles were compared between the 20 and 30 °C treatments at 0.5 mM nitrate before and after nitrate depletion and bicarbonate trigger, the dominant species of FAMEs were saturated and unsaturated C16 (hexadecanoic) and C18 (octadecanoic) FAMEs (Fig. 9). Hodgskiss et al. [2] determined that PW95, when grown in CBM water amended with 0.5 mM of initial nitrate, produced a higher amount of C:18 unsaturated acids and lower amounts of C:16 FAMEs in comparison with other reported algae. These results indicate that the FAME profile of PW95 can be manipulated with changes in culture conditions. Moreover, in comparison with other oleaginous algae that contain substantial amounts of lighter (C12–C14) and heavier (C20–C22) species, PW95 TAGs appear to be dominated by C16 and C18 fatty acids that are more common to profiles of vegetable oil fatty acids profiles from conventional biofuel producers [58]. These results suggest that PW95 could be a potential source of C16/C18 feedstock.

4. Conclusions

PW95 is a novel sporulating green microalga that can grow and produce lipids with limited input resources, and this is the first report of this type of environmental isolate for biomass and biofuel applications with standardized growth medium. The present study indicated that the most promising condition for growth and biofuel production was the

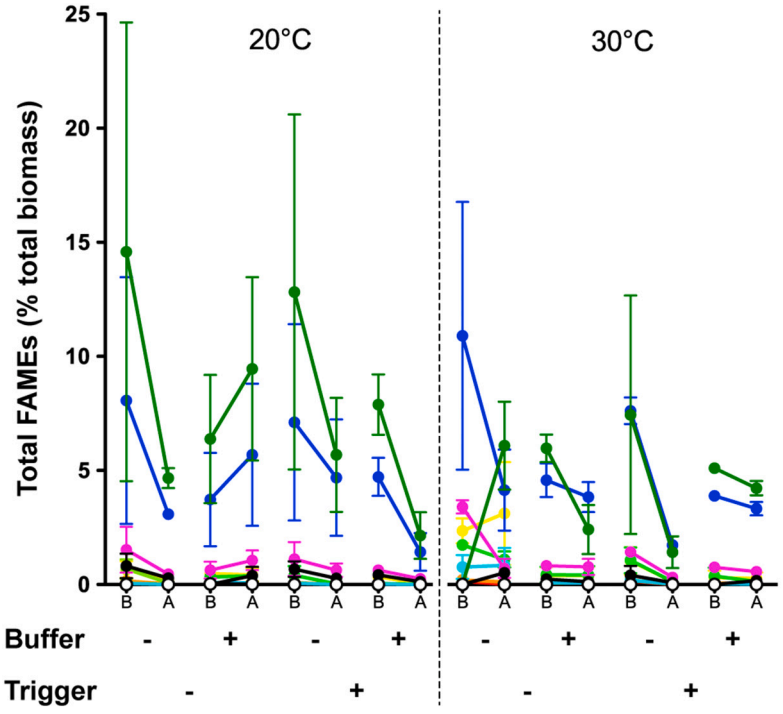

Fig. 9. PW95 FAMEs profile comparison between 20 °C and 30 °C for treatments at 0.5 mM. The x-axis labels make a distinction between FAMEs before (designated B) and after nitrate depletion and bicarbonate trigger (designated A). Treatments that included the use of a buffer and the bicarbonate trigger are represented by the plus sign (+). Treatments without buffer and bicarbonate trigger are represented by the negative sign (−). Bicarbonate trigger, if employed, was added just prior to the onset of nitrate depletion. Error bars represent the standard error of the mean of two biological independent replicates.

combination of higher temperature (30 °C) and lower nitrate level (0.5 mM) without the use of a buffer or bicarbonate trigger. These results suggest an important interaction between low nitrate levels, temperature, and elevated pH for trade-offs between biomass and lipid production in PW95. The culture condition 30 °C_0.5 Nitrate_No Buffer_No trigger showed a fast growth rate (0.80 d^{-1}), high maximum daily cell number (5.30 × 10^6 cells/mL) in 4 days of cultivation, elevated total FAMEs before and after nitrate depletion (27% and 20%) and the highest biofuel productivity (16 mg/L/day and 15 mg/L/day, respectively). Under these conditions, PW95 produced predominantly the optimal FA species (saturated and unsaturated C16 and C18) for biofuel applications. As previously reported, PW95 accumulates lipids in amended low-quality water at 20 °C and the present study demonstrated that PW95 can accumulate lipids at 20 and 30 °C in standardized media with low initial concentrations of nitrate (~17% of standard BBM) and no buffer or bicarbonate addition.

Supplementary data to this article can be found online at https://doi.org/10.1016/j.algal.2020.102148.

Disclaimer

All data generated or analyzed during this study are included in the main text or supplementary information of this publication. Any opinions, findings, conclusions or recommendations expressed herein are those of the authors and do not necessarily reflect the views of the Department of Energy (DOE) or the National Science Foundation (NSF). Any use of trade, firm, or product names is for descriptive purposes only and does not imply endorsement by the U.S. Government.

Authors' individual contributions

Luisa Corredor: Investigation, formal analysis, writing -original draft; **Elliott P. Barnhart**: resources, writing – review & editing; **Al Parker**: validation; writing-review & editing; **Robin Gerlach**: resources, project administration, writing – review & editing, funding acquisition; **Matthew W. Fields**: conceptualization, formal analysis, writing- review & editing, supervision, funding acquisition.

Statement of informed consent

No conflicts, informed consent, or human or animal rights are applicable to this study.

Author statement

All authors have seen and approved the final version of the manuscript being submitted. The article is the authors' original work, hasn't received prior publication and isn't under consideration for publication elsewhere.

Declaration of competing interest

The authors declare that they have no known competing financial interests or personal relationships that could have appeared to influence the work reported in this paper.

Acknowledgements

The authors would like to thank the Montana State University Algal Biofuel group for helpful discussion, collaboration and support. The Center for Biofilm Engineering staff: Betsey Pitts for microscopy assistance; Ann Willis, Dr. Kristen Brileya and Sara Altenburg for instrumentation and logistic assistance; Jill Story for graphics assistance. Dr. Benjamin Wheaton for editorial and graphics assistance. The authors would like to acknowledge the U.S. Geological Survey's Energy Resources Program which provided access to the field site to collect water samples for PW95's isolation. Funding was provided by the National Science Foundation under NSF-CHE-1230632 and the Department of Energy under BETO (DE-EE0005993 and DE-EE0008247). Partial support for L. Corredor was provided by the Fulbright Scholarship Program. This work was performed in part at the Montana Nanotechnology Facility (NNCI member supported by NSF ECCS-1542210).

References

[1] M.I. Khan, J.H. Shin, J.D. Kim, The promising future of microalgae: current status, challenges, and optimization of a sustainable and renewable industry for biofuels, feed, and other products, Microb. Cell Factories 17 (2018) 1–21, https://doi.org/10.1186/s12934-018-0879-x.

[2] L.H. Hodgskiss, J. Nagy, E.P. Barnhart, A.B. Cunningham, M.W. Fields, Cultivation of a native alga for biomass and biofuel accumulation in coal bed methane production water, Algal Res. 19 (2016) 63–68, https://doi.org/10.1016/J.ALGAL.2016.07.014.

[3] N.K. Singh, A.K. Upadhyay, U.N. Rai, Algal Technologies for Wastewater Treatment and Biofuels Production: An Integrated Approach for Environmental Management, in: Algal Biofuels, Springer International Publishing, Cham, 2017, pp. 97–107, https://doi.org/10.1007/978-3-319-51010-1_5.

[4] Z.T. Fica, R.C. Sims, Algae-based biofilm productivity utilizing dairy wastewater: effects of temperature and organic carbon concentration, J. Biol. Eng. 10 (2016) 1–7, https://doi.org/10.1186/s13036-016-0039-y.

[5] M.W. Fields, A. Hise, E.J. Lohman, T. Bell, R.D. Gardner, L. Corredor, K. Moll, B. M. Peyton, G.W. Characklis, R. Gerlach, Sources and resources: importance of nutrients, resource allocation, and ecology in microalgal cultivation for lipid accumulation, Appl. Microbiol. Biotechnol. 98 (2014) 4805–4816, https://doi.org/10.1007/s00253-014-5694-7.

[6] Z. Chen, L. Wang, S. Qiu, S. Ge, Determination of microalgal lipid content and fatty acid for biofuel production, Biomed. Res. Int. 2018 (2018) 1503126, https://doi.org/10.1155/2018/1503126.

[7] L.M.L. Laurens, M. Chen-Glasser, J.D. McMillan, A perspective on renewable bioenergy from photosynthetic algae as feedstock for biofuels and bioproducts, Algal Res. 24 (2017) 261–264, https://doi.org/10.1016/J.ALGAL.2017.04.002.

[8] O.M. Adeniyi, U. Azimov, A. Burluka, Algae biofuel: current status and future applications, Renew. Sust. Energ. Rev. 90 (2018) 316–335, https://doi.org/10.1016/J.RSER.2018.03.067.

[9] E. Lozoya-Gloria, X. Morales-de la Cruz, T.A. Ozawa-Uyeda, The Colonial Microalgae *Botryococcus braunii* as Biorefinery, in: Microalgae - From Physiol. to Appl., 2019: p. 13. doi:https://doi.org/10.1016/j.colsurfa.2011.12.014.

[10] M. Pawlita-Posmyk, M. Wzorek, M. Płaczek, The influence of temperature on algal biomass growth for biogas production, MATEC Web Conf. 240 (2018) 4–10, https://doi.org/10.1051/matecconf/201824004008.

[11] F. Han, W. Wang, Y. Li, G. Shen, M. Wan, J. Wang, Changes of biomass, lipid content and fatty acids composition under a light–dark cyclic culture of Chlorella pyrenoidosa in response to different temperature, Bioresour. Technol. 132 (2013) 182–189, https://doi.org/10.1016/J.BIORTECH.2012.12.175.

[12] F. Mus, J.-P. Toussaint, K.E. Cooksey, M.W. Fields, R. Gerlach, B.M. Peyton, R. P. Carlson, Physiological and molecular analysis of carbon source supplementation and pH stress-induced lipid accumulation in the marine diatom Phaeodactylum tricornutum, Appl. Microbiol. Biotechnol. 97 (2013) 3625–3642, https://doi.org/10.1007/s00253-013-4747-7.

[13] L. Xia, H. Yang, Q. He, C. Hu, Physiological responses of freshwater oleaginous microalgae Desmodesmus sp. NMX451 under nitrogen deficiency and alkaline pH-induced lipid accumulation, J. Appl. Phycol. 27 (2014) 649–659. doi:https://doi.org/10.1007/s10811-014-0371-x.

[14] T. Menegol, A.B. Diprat, E. Rodrigues, R. Rech, Effect of temperature and nitrogen concentration on biomass composition of heterochlorella luteoviridis, Food Sci. Technol. 37 (2017) 28–37, https://doi.org/10.1590/1678-457X.13417.

[15] T.C. Pedersen, R.D. Gardner, R. Gerlach, B.M. Peyton, Assessment of Nannochloropsis gaditana growth and lipid accumulation with increased inorganic carbon delivery, J. Appl. Phycol. 30 (2018) 2155–2166, https://doi.org/10.1007/s10811-018-1470-x.

[16] R. Srinivasan, A. Mageswari, P. Subramanian, C. Suganthi, A. Chaitanyakumar, V. Aswini, & Kodiveri, M. Gothandam, Bicarbonate supplementation enhances growth and biochemical composition of *Dunaliella salina* V-101 by reducing oxidative stress induced during macronutrient deficit conditions OPEN, Nat. Sci. RePoRTS. 8 (2018) 6972. doi:https://doi.org/10.1038/s41598-018-25417-5.

[17] J.J. Kozich, S.L. Westcott, N.T. Baxter, S.K. Highlander, P.D. Schloss, Development of a dual-index sequencing strategy and curation pipeline for analyzing amplicon sequence data on the MiSeq Illumina sequencing platform, Appl. Environ. Microbiol. 79 (2013) 5112–5120, https://doi.org/10.1128/AEM.01043-13.

[18] K.E. Cooksey, J.B. Guckert, S.A. Williams, P.R. Callis, Fluorometric determination of the neutral lipid content of microalgal cells using Nile Red, J. Microbiol. Methods 6 (1987) 333–345, https://doi.org/10.1016/0167-7012(87)90019-4.

[19] S.F. Altschul, W. Gish, W. Miller, E.W. Myers, D.J. Lipman, Basic local alignment search tool, J. Mol. Biol. 215 (1990) 403–410, https://doi.org/10.1016/S0022-2836(05)80360-2.

[20] T.J. White, T. Bruns, S. Lee, J. Taylor, Amplification and direct sequencing of fungal ribosomal RNA genes for phylogenetics, PCR Protoc. (1990) 315–322, https://doi.org/10.1016/B978-0-12-372180-8.50042-1.

[21] E.P. Nawrocki, Structural RNA Homology Search and Alignment Using Covariance Models. http://eddylab.org/publications/Nawrocki09b/Nawrocki09b-phdthesis.pdf, 2009. (Accessed 13 June 2019).
[22] S. Capella-Gutiérrez, J.M. Silla-Martínez, T. Gabaldón, trimAl: a tool for automated alignment trimming in large-scale phylogenetic analyses, Bioinforma. Appl. NOTE. 25 (2009) 1972–1973. doi:https://doi.org/10.1093/bioinformatics/btp348.
[23] F. Ronquist, M. Teslenko, P. Van Der Mark, D.L. Ayres, A. Darling, S.H.¨ Ohna, B. Larget, L. Liu, M.A. Suchard, J.P. Huelsenbeck, Software for Systematics and Evolution MrBayes 3.2: Efficient Bayesian Phylogenetic Inference and Model Choice Across a Large Model Space, Syst. Biol. 61 (2012) 539–542. doi:https://doi.org/10.1093/sysbio/sys029.
[24] I. Letunic, P. Bork, Interactive Tree of Life (iTOL) v4: Recent Updates and New Developments, Nucleic Acids Res, 2019, https://doi.org/10.1093/nar/gkz239.
[25] K. Katoh, K. Misawa, K.-I. Kuma, T. Miyata, MAFFT: a novel method for rapid multiple sequence alignment based on fast Fourier transform, Nucleic Acids Res. 30 (2002) 3059–3066. https://www.ncbi.nlm.nih.gov/pmc/articles/PMC135756/pdf/gkf436.pdf. (Accessed 4 September 2019).
[26] E.J. Lohman, R.D. Gardner, T. Pedersen, B.M. Peyton, K.E. Cooksey, R. Gerlach, Optimized inorganic carbon regime for enhanced growth and lipid accumulation in Chlorella vulgaris, Biotechnol. Biofuels. 8 (2015) 82, https://doi.org/10.1186/s13068-015-0265-4.
[27] R.J. Ritchie, Consistent sets of spectrophotometric chlorophyll equations for acetone, methanol and ethanol solvents, Photosynth. Res. 89 (2006) 27–41, https://doi.org/10.1007/s11120-006-9065-9.
[28] J. Valenzuela, R.P. Carlson, R. Gerlach, K. Cooksey, B.M. Peyton, B. Bothner, M. W. Fields, Nutrient resupplementation arrests bio-oil accumulation in Phaeodactylum tricornutum, Appl. Microbiol. Biotechnol. 97 (2013) 7049–7059, https://doi.org/10.1007/s00253-013-5010-y.
[29] W. Chen, C. Zhang, L. Song, M. Sommerfeld, Q. Hu, A high throughput Nile red method for quantitative measurement of neutral lipids in microalgae, J. Microbiol. Methods 77 (2009) 41–47, https://doi.org/10.1016/J.MIMET.2009.01.001.
[30] M.J. Griffiths, R.P. van Hille, S.T.L. Harrison, Selection of direct Transesterification as the preferred method for assay of fatty acid content of microalgae, Lipids. 45 (2010) 1053–1060, https://doi.org/10.1007/s11745-010-3468-2.
[31] E.J. Lohman, R.D. Gardner, L. Halverson, R.E. Macur, B.M. Peyton, R. Gerlach, An efficient and scalable extraction and quantification method for algal derived biofuel, J. Microbiol. Methods 94 (2013) 235–244, https://doi.org/10.1016/j.mimet.2013.06.007.
[32] J.C Pinheiro, M.B Douglas, Mixed Effects Models in S and S-Plus, Springer, New York, 2000. M.J. doi:https://doi.org/10.1007/0-387-22747-4_4.
[33] J. Neter, M.H Kutner, C.J Nachtsheim, W. Wasserman, Applied Linear Statistical Models, Irwin, Chicago, 1990.
[34] M. Hamilton, G. Hamilton, D. Goeres, A. Parker, Guidelines for the statistical analysis of a collaborative study of a laboratory disinfectant product performance test method, JAOAC International. 96 (2013) 1138–1151.
[35] L.E. Shubert, Nonmotile Coccoid and Colonial Green Algae, in: Freshw, Academic Press, Algae North Am. Ecol. Classif, 2002, pp. 253–309, https://doi.org/10.1016/B978-012741550-5/50008-8.
[36] Q. Béchet, M. Laviale, N. Arsapin, H. Bonnefond, O. Bernard, Modeling the impact of high temperatures on microalgal viability and photosynthetic activity, Biotechnol. Biofuels. 10 (2017) 136, https://doi.org/10.1186/s13068-017-0823-z.
[37] H. Jiang, K. Gao, Effects of lowering temperature during culture on the production of polyunsaturated fatty acids in the marine diatom phaeodactylum tricornutum (bacillariophyceae)1, J. Phycol. 40 (2004) 651–654, https://doi.org/10.1111/j.1529-8817.2004.03112.x.
[38] D.P. Kurpan Nogueira, A.F. Silva, O.Q.F. Araújo, R.M. Chaloub, Impact of temperature and light intensity on triacylglycerol accumulation in marine microalgae, Biomass Bioenergy 72 (2015) 280–287, https://doi.org/10.1016/J.BIOMBIOE.2014.10.017.
[39] L. Aleya, A. Dauta, C.S. Reynolds, Endogenous regulation of the growth-rate responses of a spring-dwelling strain of the freshwater alga, Chlorella minutissima, to light and temperature, Eur. J. Protistol. 47 (2011) 239–244, https://doi.org/10.1016/J.EJOP.2011.05.003.
[40] P.L. Show, M.S.Y. Tang, D. Nagarajan, T.C. Ling, C.W. Ooi, J.S. Chang, A holistic approach to managing microalgae for biofuel applications, Int. J. Mol. Sci. 18 (2017). doi:https://doi.org/10.3390/ijms18010215.
[41] S.P. Singh, P. Singh, Effect of temperature and light on the growth of algae species: a review, Renew. Sust. Energ. Rev. 50 (2015) 431–444, https://doi.org/10.1016/j.rser.2015.05.024.
[42] K.M. Moll, R.D. Gardner, E.O. Eustance, R. Gerlach, B.M. Peyton, Combining multiple nutrient stresses and bicarbonate addition to promote lipid accumulation in the diatom RGd-1, Algal Res. 5 (2014) 7–15, https://doi.org/10.1016/J.ALGAL.2014.04.002.
[43] L.-S. Zhao, K. Li, Q.-M. Wang, X.-Y. Song, H.-N. Su, B.-B. Xie, X.-Y. Zhang, F. Huang, X.-L. Chen, B.-C. Zhou, Y.-Z. Zhang, Nitrogen starvation impacts the photosynthetic performance of Porphyridium cruentum as revealed by chlorophyll a fluorescence, Sci. Rep. 7 (2017) 8542, https://doi.org/10.1038/s41598-017-08428-6.
[44] J. Valenzuela, A. Mazurie, R.P. Carlson, R. Gerlach, K.E. Cooksey, B.M. Peyton, M. W. Fields, Potential role of multiple carbon fixation pathways during lipid accumulation in Phaeodactylum tricornutum, Biotechnol. Biofuels. 5 (2012) 40, https://doi.org/10.1186/1754-6834-5-40.
[45] Y. Li, M. Horsman, B. Wang, N. Wu, C.Q. Lan, Effects of nitrogen sources on cell growth and lipid accumulation of green alga Neochloris oleoabundans, Appl. Microbiol. Biotechnol. 81 (2008) 629–636, https://doi.org/10.1007/s00253-008-1681-1.
[46] R. Ramaraj, D.D.-W. Tsai, P.H. Chen, Chlorophyll is not accurate measurement for algal biomass, Chiang Mai J. Sci. 40 (2013) 1–9. http://it.science.cmu.ac.th/ejournal/. (Accessed 1 July 2019).
[47] N.A. Eckardt, A new chlorophyll degradation pathway, Plant Cell 21 (2009) 700, https://doi.org/10.1105/tpc.109.210313.
[48] Y.M. Zhang, H. Chen, C.L. He, Q. Wang, Nitrogen starvation induced oxidative stress in an oil-producing green alga Chlorella sorokiniana C3, PLoS One 8 (2013) 1–12, https://doi.org/10.1371/journal.pone.0069225.
[49] M. Ellegaard, S. Ribeiro, The long-term persistence of phytoplankton resting stages in aquatic "seed banks," Biol. Rev. 93 (2018) 166–183. doi:https://doi.org/10.1111/brv.12338.
[50] I. Pancha, K. Chokshi, T. Ghosh, C. Paliwal, R. Maurya, S. Mishra, Bicarbonate supplementation enhanced biofuel production potential as well as nutritional stress mitigation in the microalgae Scenedesmus sp. CCNM 1077, Bioresour. Technol. 193 (2015) 315–323. doi:https://doi.org/10.1016/j.biortech.2015.06.107.
[51] R.D. Gardner, E.J. Lohman, K.E. Cooksey, R. Gerlach, B.M. Peyton, Cellular cycling, carbon utilization, and photosynthetic oxygen production during bicarbonate-induced triacylglycerol accumulation in a Scenedesmus sp, Energies. 6 (2013) 6060–6607, https://doi.org/10.3390/en6116060.
[52] D.A. White, A. Pagarette, P. Rooks, S.T. Ali, The effect of sodium bicarbonate supplementation on growth and biochemical composition of marine microalgae cultures, J. Appl. Phycol. 25 (2013) 153–165, https://doi.org/10.1007/s10811-012-9849-6.
[53] E. Eustance, R.D. Gardner, K.M. Moll, J. Menicucci, R. Gerlach, B.M. Peyton, Growth, nitrogen utilization and biodiesel potential for two chlorophytes grown on ammonium, nitrate or urea, J. Appl. Phycol. 25 (2013) 1663–1677, https://doi.org/10.1007/s10811-013-0008-5.
[54] R.D. Gardner, K.E. Cooksey, F. Mus, R. Macur, K. Moll, E. Eustance, R.P. Carlson, R. Gerlach, M.W. Fields, B.M. Peyton, Use of sodium bicarbonate to stimulate triacylglycerol accumulation in the chlorophyte Scenedesmus sp. and the diatom *Phaeodactylum tricornutum*, J. Appl. Phycol. 24 (2012) 1311–1320. doi:https://doi.org/10.1007/s10811-011-9782-0.
[55] X. Wang, H.K. Fosse, K. Li, M.S. Chauton, O. Vadstein, K.I. Reitan, Influence of nitrogen limitation on lipid accumulation and EPA and DHA content in four marine microalgae for possible use in aquafeed, Front. Mar. Sci. 6 (2019) 1–10, https://doi.org/10.3389/fmars.2019.00095.
[56] R.D. Gardner, E. Lohman, R. Gerlach, K.E. Cooksey, B.M. Peyton, Comparison of CO2 and bicarbonate as inorganic carbon sources for triacylglycerol and starch accumulation in Chlamydomonas reinhardtii, Biotechnol. Bioeng. 110 (2013) 87–96, https://doi.org/10.1002/bit.24592.
[57] G. Breuer, W.A.C. Evers, J.H. de Vree, D.M.M. Kleinegris, D.E. Martens, R.H. Wijffels, P.P. Lamers, Analysis of fatty acid content and composition in microalgae., J. Vis. Exp. (2013). doi:https://doi.org/10.3791/50628.
[58] S.K. Hoekman, A. Broch, C. Robbins, E. Ceniceros, M. Natarajan, Review of biodiesel composition, properties, and specifications, Renew. Sust. Energ. Rev. 16 (2012) 143–169, https://doi.org/10.1016/J.RSER.2011.07.143.